

Synthesis and Thermal Decomposition Mechanism of Rare Earth (RE=La, Y, Gd) Salicylates

LI, Liang-Chao^{*a}(李良超) ZHOU, Xiang-Chun^b(周享春) ZHENG, Ren-Wei^a(郑人卫)

^a Department of Chemistry, Institute of Physical Chemistry, Zhejiang Normal University, Jinhua, Zhejiang, 321004, China

^b College of Chemistry and Environmental Engineering, Yangtze University, Jingzhou, Hubei 434102, China

The rare earth (RE=La, Y, Gd) salicylates were synthesized by the rheological phase reaction method. The complexes were characterized by elemental analysis, infrared spectra (IR), X-ray powder diffraction (XRD) and thermal gravity analysis (TG). They can be represented by general formula RE(HSal)₃ (RE=La, Y, Gd; HSal=C₆H₄(OH)COO). The crystals of them are monoclinic and have layered structure. The mechanism of thermal decomposition of rare earth salicylates was studied by using TG, DTA, IR and gas chromatography-mass spectrometry (GC-MS). The thermal decomposition of the rare earth salicylates in nitrogen gas proceeded in three stages: firstly, they were decomposed to form RE₂(Sal)₃ (Sal=C₆H₄OCOO) and salicylic acid; then, RE₂(Sal)₃ were decomposed further to form RE₂O(CO₃)₂ and some organic compounds; finally, RE₂O(CO₃)₂ were decomposed to form rare earth metal oxides (RE₂O₃) and carbon dioxide. The organic compounds obtained from the second step of the reaction are mainly dibenzofuran, xanthenone, 6*H*-benzo[*c*]chromen-6-one, 6-phenyl-6*H*-benzo[*c*]chromene, and 1,3-diphenyl-1, 3-dihydro-2-benzofuran.

Keywords rare earth, salicylate, rheological phase, thermal decomposition

Introduction

Rare earth salicylates are a kind of important compounds. The coordination compounds formed by rare earth salts and salicylic acid have unusual structures and interesting luminescent properties. By means of forming conjugated complexes, rare earth metals and salicylic acid can form net or polymer to change their luminescent properties. Some rare earth complexes have been applied to agriculture as light-transferring materials. The thermal decomposition of the transition metal salicylates has been reported in air¹⁻³ and inert atmosphere^{4,5} However, no other detailed study has been reported on the thermal decomposition reaction mechanism of rare earth salicylates in inert atmosphere, and it was found that many aromatic organic compounds were formed, such as benzophenone and anthraquinone, 6*H*-benzo[*c*]-chromen-6-one and dibenzofuran.^{6,7} Some organic compounds have been prepared by means of thermal decomposition of these complexes, which were characterized by elemental analysis, IR, X-ray powder diffraction and gas chromatography-mass spectrometry. The thermal decomposition mechanism of the complexes was investigated, and it was expected to obtain a new path of synthesizing aryl compounds.

Experimental

Preparation of samples

The purity of the starting materials RE₂O₃ (RE=La, Y, Gd) is 99.95% and salicylic acid is analytical reagent grade. These reagents and solvent were used without further purification.

RE₂O₃ and salicylic acid are fully mixed by grinding in a molar ratio of 1 : 6, and a proper amount of water was added to prepare solid-liquid rheological state (solid-liquid rheological state is a kind of semi-solid in which solid particles and liquid substance are uniformly distributed). It was reacted for 12 h in a closed container at 80—100 °C. Subsequently, the samples were washed 3—4 times with anhydrous ethanol or ethyl ether and dried at 100 °C for 4 h. The anhydrous rare earth salicylates were obtained.

Characterization of samples

The contents of carbon and hydrogen were determined by a Perkin-Elmer 240B element analyzer. The contents of RE were determined by titration with EDTA. The density of samples was determined with specific gravity bottle (cyclohexane used as displacer). The infrared spectra of the samples in KBr pellets were recorded on a Nicolet 550 FT-IR spectrometer in the range 4000—400 cm⁻¹. The X-ray diffraction pattern

* E-mail: lilc58715@sina.com.cn

Received March 1, 2004; revised April 28, 2004; accepted July 13, 2004.

Project supported by the Natural Science Foundation of Hubei Education Committee (No. 2003A010) and Introducing Able Person Foundation of Zhejiang Normal University.

was obtained with a Rigaku D/MAX-RA model X-ray diffractometer with a Ni-filler and graphite monochromator, and Cu $K\alpha_1$ radiation ($\lambda=0.15405$ nm). The TG and DTA curves of the samples (6.2—8.7 mg) were recorded with a Shimadzu model DT-40 thermal analyzer in N_2 (flow rate $40 \text{ mL}\cdot\text{min}^{-1}$) at a heating ratio of $20 \text{ }^\circ\text{C}\cdot\text{min}^{-1}$ from room temperature to $900 \text{ }^\circ\text{C}$, platinum cups were used as sample and reference holders, and alumina was used as a reference material.

Collection and characterization of decomposition products

According to the data of DTA and TG, the samples of 3—4 g were decomposed in an atmosphere of N_2 in tubular furnace at $400 \text{ }^\circ\text{C}$ for 5 h, and their products were collected.⁷ The chromatography and mass spectrograms of the gas condensates from thermal decomposition of samples were recorded on a VG analytical 7070 E-HF gas chromatography-mass spectrometer. GC-MS was conducted on a Beijing KYKY GC/MS-DS2 computer data system with an HP 5790A gas chromatography and an OV1701 elastic quartz capillary column (0.32 mm inside diameter and 30 m in length). Gas chromatography was performed in the conditions: He as the carrier gas, pre-column pressure 880 kPa, starting temperature $80 \text{ }^\circ\text{C}$, heating rate $8 \text{ }^\circ\text{C}\cdot\text{min}^{-1}$, final temperature $290 \text{ }^\circ\text{C}$, and mass spectrometry: EI ionization manner, ion source temperature $200 \text{ }^\circ\text{C}$, accelerating voltage 6 kV, electron energy 70 eV, and scanning range 45—800 m/z .

Results and discussion

Elemental analysis

The analysis data of the element content are presented in Table 1. The products can be represented by general formula $\text{RE}(\text{OHC}_6\text{H}_4\text{COO})_3$. The experimental data are in a good accord with the calculated values (in parenthesis).

Table 1 Element analysis data of rare earth salicylates (%)

Compound	RE	C	H
Lanthanum salicylate	25.30 (25.24)	45.50 (45.84)	3.01 (2.75)
Yttrium salicylate	17.56 (17.77)	50.93 (50.42)	2.84 (3.01)
Gadolinium salicylate	26.65 (26.81)	44.81 (44.35)	2.48 (2.66)

XRD data

The cell parameters of $\text{RE}(\text{C}_6\text{H}_4\text{OHCOO})_3$ were calculated from XRD data and presented in Table 2. Each of them belongs to monoclinic system. All lines of the X-ray powder diffraction pattern were indexed by using these crystal parameters. The strongest diffraction plane ($I/I_1=100$) is (1 0 0) crystal plane, and the rest planes are much weak. Inferring this information, RE atoms were located in (1 0 0) crystal plane and benzene ring in either side, and have layered structure.

Table 2 Crystal parameters of $\text{RE}(\text{HSal})_3$

Compound	La(HSal) ₃	Y(HSal) ₃	Gd(HSal) ₃
a/nm	2.1601	1.4988	1.8584
b/nm	1.3802	0.8613	1.0196
c/nm	0.3810	1.0883	0.6837
$\beta/^\circ$	97.11	92.15	93.84
V/nm^3	1.1272	1.4042	1.2955
Z	2	2	2
$D_{\text{calcd}}/(\text{g}\cdot\text{cm}^{-3})$	1.6210	1.5792	1.5986
$D_{\text{expl}}/(\text{g}\cdot\text{cm}^{-3})$	1.6530	1.5827	1.5954

IR spectra

Figure 1 shows the IR spectra of $\text{La}(\text{HSal})_3$. The IR spectra of $\text{Y}(\text{HSal})_3$ and $\text{Gd}(\text{HSal})_3$ are the same as those of $\text{La}(\text{HSal})_3$ approximately. In Figure 1, the sharp absorption band at 1620, 1590, 1512 and 1465 cm^{-1} can be assigned to the C—C stretching vibration of the benzene ring, and the strong band at 1238 cm^{-1} to the C—O bond. The sharp and strong absorption band at $3300\text{—}3170 \text{ cm}^{-1}$ can be contributed to the OH stretching vibration of the benzene ring. The bands for COO occur at 1556 cm^{-1} [$\text{La}(\text{HSal})_3$], 1543 cm^{-1} [$\text{Y}(\text{HSal})_3$] and 1564 cm^{-1} [$\text{Gd}(\text{HSal})_3$] for anti-symmetric vibration and 1420 cm^{-1} [$\text{La}(\text{HSal})_3$], 1413 cm^{-1} [$\text{Y}(\text{HSal})_3$] and 1350 cm^{-1} ($\text{Gd}(\text{HSal})_3$) for symmetric vibration of the $\text{La}(\text{HSal})_3$, $\text{Y}(\text{HSal})_3$ and $\text{Gd}(\text{HSal})_3$, respectively. The difference between ν_a (OCO) and ν_s (OCO) vibration of the carboxyl group reaches a value of $210\text{—}130 \text{ cm}^{-1}$, revealing that the carboxyl group is coordinated to RE atom in a symmetric bidentate or an asymmetric bidentate bridging coordinates.⁸

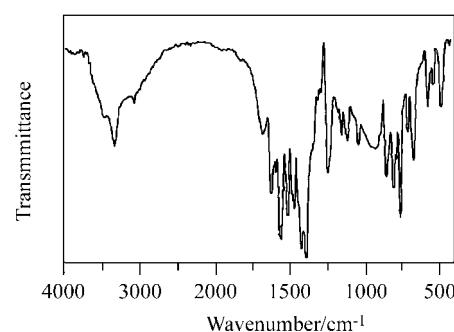


Figure 1 Infrared spectrum of $\text{La}(\text{HSal})_3$.

Thermal analysis

Figure 2 shows the TG and DTA curves of $\text{La}(\text{HSal})_3$. The TG and DTA curves of $\text{Y}(\text{HSal})_3$ and $\text{Gd}(\text{HSal})_3$ are the same as those of $\text{La}(\text{HSal})_3$ approximately. The TG curve has three stages, and the weight of loss and the temperature range in each stage are given in Table 3. These experimental data are in good agreement with the calculated values (in parentheses). The DTA curve exhibits five endothermic peaks: The first peak can be assigned to $\text{La}(\text{HSal})_3 \rightarrow \text{La}_2(\text{Sal})_3$ and sublimating of H_2Sal at $203.9 \text{ }^\circ\text{C}$. The second peak may be

due to sublimating of polycyclic aromatic hydrocarbon at 267.6 °C. The third peak can be assigned to $\text{La}_2(\text{Sal})_3$ decomposition to $\text{La}_2\text{O}(\text{CO}_3)_2$ at 439.2 °C. The final two peaks correspond to $\text{La}_2\text{O}(\text{CO}_3)_2 \rightarrow \text{La}_2\text{O}_2\text{CO}_3$ and $\text{La}_2\text{O}_2\text{CO}_3 \rightarrow \text{La}_2\text{O}_3$ at 693.2 and 767.6 °C, respectively.

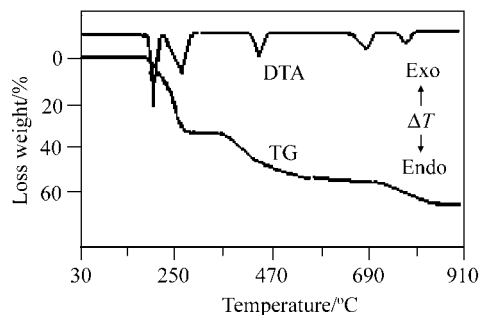


Figure 2 TG and DTA curves of $\text{La}(\text{Hsal})_3$.

Table 3 Loss weight and the decomposition temperature range of $\text{RE}(\text{HSal})_3$

Compound	Temp. range/°C	Loss weight/%	Remnant
$\text{La}(\text{HSal})_3$	179.8—328.9	36.87 (37.65)	$\text{La}_2(\text{Sal})_3$
	328.9—439.2	24.02 (24.74)	$\text{La}_2\text{O}(\text{CO}_3)_2$
	615.5—848.4	8.43 (8.00)	La_2O_3
$\text{Y}(\text{HSal})_3$	198.4—341.5	40.75 (41.41)	$\text{Y}_2(\text{Sal})_3$
	341.5—570.3	27.66 (27.21)	$\text{Y}_2\text{O}(\text{CO}_3)_2$
	626.9—794.7	8.38 (8.80)	Y_2O_3
$\text{Gd}(\text{HSal})_3$	205.3—330.1	37.16 (36.43)	$\text{Gd}_2(\text{Sal})_3$
	330.1—445.8	23.74 (23.93)	$\text{Gd}_2\text{O}(\text{CO}_3)_2$
	625.0—850.7	8.16 (7.74)	Gd_2O_3

GC-MS analysis of gas phase products

The condensates of gas phase products as dark red thick matter were collected from thermal decomposition of $\text{RE}_2(\text{Sal})_3$ at 400 °C in N_2 atmosphere and immersed in acetone. The insoluble matter in acetone is a colorless crystal. Its IR spectrum (Figure 3) is in a good accord with the standard IR spectra of xanthenone (IR, the Sadler Standard Spectra No. 18091 K). The soluble matter was dried at 90 °C in order to get rid of acetone. The analytical results of GC-MS of the condensates of gas phase products from $\text{La}_2(\text{Sal})_3$ are presented in Table 4.

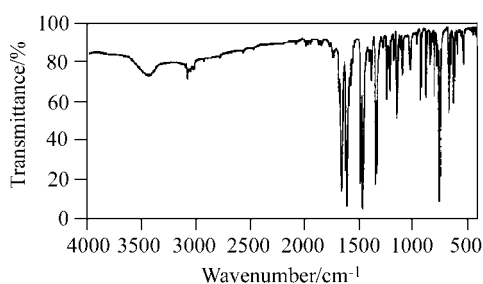


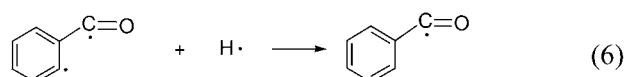
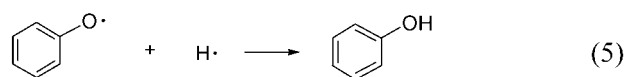
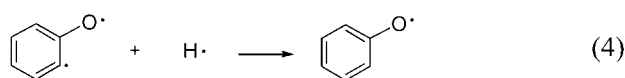
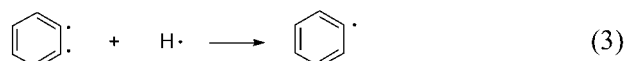
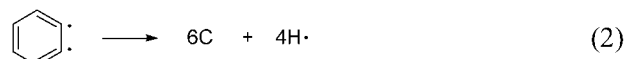
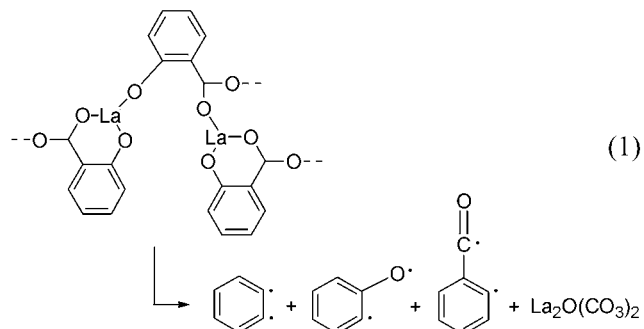
Figure 3 IR spectra of xanthenone.

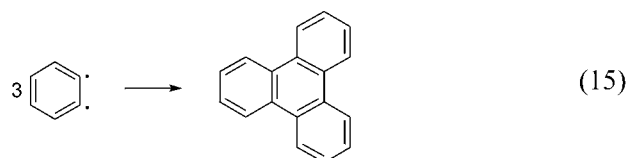
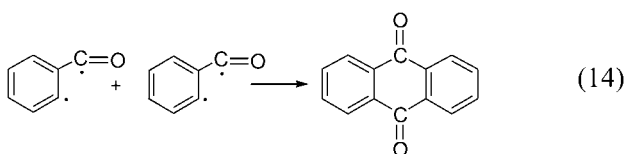
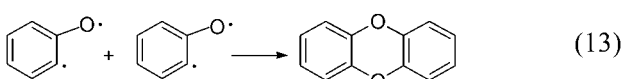
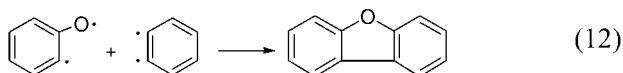
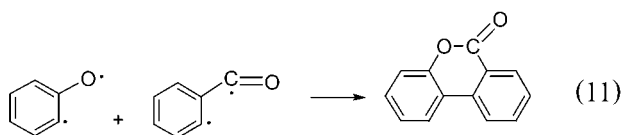
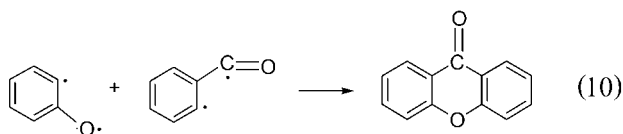
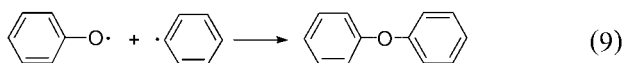
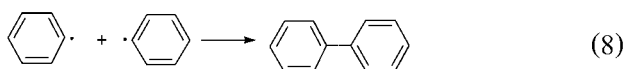
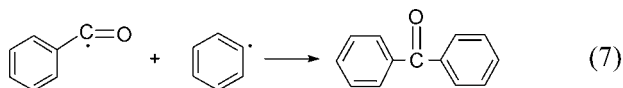
It can be seen that gas phase products of thermal decomposition include mainly dibenzofuran, xanthenone, 6*H*-benzo[*c*]chromen-6-one, 6-phenyl-6*H*-benzo[*c*]chromene and 1,3-diphenyl-1,3-dihydro-2-benzofuran.

Table 4 Analytical results of GC-MS for gas phase products

No.	Compound	Molecular weight	Hold time/min	Content/%
1	Phenol	94	8.295	2.64
2	Biphenyl	155	18.165	0.58
3	Fluorene	166	21.923	0.72
4	Dibenzofurane	168	19.098	23.47
5	Biphenyl ether	170	19.694	3.16
6	Fluorenone	180	20.639	0.26
7	Xanthenone	182	22.983	9.38
8	Xanthenone	196	27.117	28.06
9	6 <i>H</i> -benzo[<i>c</i>]chromen-6-one	196	28.556	13.14
10	Triphenylene	228	36.373	0.16
11	9-Phenyl-fluorene	242	30.857	0.12
12	2-Phenoxy-biphenyl	246	28.644	0.36
13	6-Phenyl-6 <i>H</i> -benzo[<i>c</i>]chromene	258	31.683	7.21
14	1,3-Diphenyl-1,3-dihydro-2-benzofuran	270	34.596	10.74

From the results in Figure 2 and Table 4, we may reveal the thermal decomposition mechanism as follows.





During the thermal decomposition of $\text{RE}_2(\text{Sal})_3$, the fracture of bond occurs chiefly in accordance with Eqs. (2)—(5), which results in forming $\cdot\text{C}_6\text{H}_4\text{O}\cdot$, $\text{C}_6\text{H}_4\text{O}\cdot$, $\cdot\text{C}_6\text{H}_4\text{C}(\text{O})\cdot$, $\text{C}_6\text{H}_4\text{C}(\text{O})\cdot$, $\cdot\text{C}_6\text{H}_4\cdot$ and $\text{C}_6\text{H}_5\cdot$ free radicals.

These free radicals reacted further to form xanthone, 6*H*-benzo[*c*]chromen-6-one, dibenzofuran, phenol, 6-phenyl-6*H*-benzo[*c*]chromene and 1,3-diphenyl-1,3-dihydro-2-benzofuran, and so on.

References

- 1 Kharitonov, Y. Y.; Tuiebakhova, Z. K. *Zh. Neorg. Khim.* **1986**, *31*, 2005.
- 2 Garcia-Oricain, J.; Fuster Camps, A. *J. Therm. Anal.* **1984**, *29*, 793.
- 3 Kharitonov, Y. Y.; Tuiebakhova, Z. K. *Zh. Neorg. Khim.* **1984**, *29*, 3030.
- 4 Sun, J. T.; Yuan, L. J.; Zhang, K. L. *Thermochim. Acta.* **1999**, *333*, 141.
- 5 Zhang, K. L.; Yuan, J. B.; Yuan, L. J.; Sun, J. T. *J. Rare Earths* **1999**, *17*, 255.
- 6 Sun, J. T.; Yuan, L. J.; Zhang, K. L.; Wang, D. L. *Thermochim. Acta* **2000**, *343*, 105.
- 7 Sun, J. T.; Zhang, K. L.; Zhang, J. M.; Qin, Z. B.; Fen, Y. L. *Chem. J. Chin. Univ.* **1992**, *13*, 1345 (in Chinese).
- 8 Pavkovic, S. F. *J. Inorg. Nucl. Chem.* **1971**, *33*, 1475.

(E0403019 SONG, J. P.)